

Hydraulic analysis with CFD numerical modeling - 3D flow of local erosion in bridge piers

Khaled Hamad, Cristina Torres

Escuela Politécnica Nacional, Ecuador

Abstract: At the Center for Research and Studies in Water Resources (CIERHI), an experimental analysis was conducted using a physical model to study the turbulence phenomena that lead to erosion around bridge piers (Chiliquinga & Pinto, 2019). The data obtained from the above-mentioned experimental model served as the calibration basis for the three-dimensional numerical modeling of the erosion around bridge piers, with the application of the FLOW-3D computational software package. After the model was calibrated, the conditions under which the physical model was established were enhanced. This was because the experimental results indicated that a deeper sand bed was required to accurately determine the maximum degree of erosion. Optimal conditions were set in the numerical model so as to obtain results free from the physical constraints present in the experimental model. In this way, the results of the maximum erosion around bridge piers were acquired. These results were then compared with the values calculated according to various empirical equations.

Key words: Scour; piers; simulation; modelling; undermining; flow 3D

1 Introduction

In the field of hydraulic engineering, river flow and associated problems, such as sediment transport, riverbed deformation, scour, and flooding, are considered the main problems facing a country. Most bridge failures are due to scour, a case in point being the 1973 U.S. Federal Highway Administration study, which determined that of 383 observed bridge failures, 97% were caused by hydraulic problems from local erosion: 25% in piers and 75% in abutments; that is, only 3% of recorded failures were due to causes unrelated to hydraulics (Fernández, 2004).

Within the Center for Research and Studies in Water Resources (CIERHI), an experimental analysis was carried out in a physical model of turbulence phenomena that cause erosion around bridge piers (Chiliquinga & Pinto, 2019). The experimental results determined that a higher sand bed was necessary to determine the maximum erosion depth. Furthermore, the channel walls of the physical model directly influenced the results because friction along the channel walls affects the velocity distribution in the central region. This phenomenon could be avoided if the experimental analysis was performed in a wide open channel (if the width is greater than 5 to 10 times the flow depth) (Chow, 2004). In the numerical model, optimal conditions were set to obtain results without the physical limitations of an experimental model, such as the height of the sediment bed and the width of the channel, which in the physical model was set with negligible friction on the walls.

2 Methodology

2.1 Physical model

(Experimental analysis in a physical model of turbulence phenomena causing erosion around bridge piers using ADV)

(Chiliquinga & Pinto, 2019).

Within the Center for Research and Studies in Water Resources (CIERHI), the turbulence phenomenon that causes the erosion and scour of solid material around a bridge pier was experimentally analyzed (Chiliquinga & Pinto, 2019). The tests were carried out in the CIERHI hydrodynamic channel, a sediment bed 2 meters long, 12 cm high was placed, occupying the total width of the one-meter channel. Two concrete piles were used in separate tests; for the first test, a square cross-section 10 cm wide was used and in the second test, a circular cross-section with a diameter of 10 cm, both piles 90 cm high. The piles were located 50 cm from the edge of the sediment bed. The location of the piles can be seen in Figure 1.



Figure 1. Location of the square and circular pile on the sand bed

The threshold movement conditions were determined experimentally and via the Shields diagram to calculate the critical initiation condition. This ensured the sand remained stationary without the pile, while allowing analysis of bed erosion around the pile caused by the structure. Experimentally, the beginning of particle movement occurred with a draft of 0.205 m. Using the Shields diagram to calculate the threshold or principle of movement, a draft of 0.21 m was determined, verifying coincident values experimentally and analytically.

The boundary conditions used in the physical model are: Flow rate 52.47 l/s, draft 0.25 m, which gives a velocity of 0.21 m/s.

The sediment used in the physical model has the following properties (Chiliquinga & Pinto, 2019):

Specific weight of sediment = 2.65 t/m^3

$D_{16} = 0,403 \text{ mm}$

$D_{50} = 0,739 \text{ mm}$

$D_{84} = 1,072 \text{ mm}$

$D_{90} = 1,142 \text{ mm}$

Representative sizes of the sediment are: diameter 0.85 mm with 20.4%, diameter 0.71 mm with 36.7% and 0.6 mm with 36.6%.

According to the size classification of sediments (sand), the group and class of sediment corresponds to coarse sand. Calculating the standard deviation of the material's particle size yields a result of 1.63 (Chiliquinga & Pinto, 2019). The

standard deviation allows determining the sample's particle size. In this case, a value less than three is obtained, which indicates that the granulometry is uniform, a typical condition in sediments for laboratory use (synthetic material).

In the physical model without piles, the conditions for the onset of movement were experimentally determined. This was achieved by varying the draft with the aid of a gate positioned downstream of the bed. The flow rate was maintained, and the height of the water was reduced until the movement of the particles began.

The threshold or beginning of particle movement was also calculated using the Shields diagram, which is generated when the bed tension and the critical tension are equal. This procedure is performed to guarantee the Clear Water condition (which means that the flow does not reach the critical velocity, and since it does not have enough force to mobilize the bed particles, there is no generalized movement; erosion could only occur if an obstacle is encountered; therefore, the only possible erosion is local). A draft was placed that does not generate particle movement without the pile since what is intended to evaluate is precisely the erosion suffered by the bed around a pile due to the presence of said structure (Chiliquinga & Pinto, 2019).

It was not possible to determine the maximum erosion results in the physical model because the scour around the square and circular piles reached 12 cm of the sand bed after four hours of testing.

2.2 Numerical model (calibration)

Computational Fluid Dynamics (CFD) uses specially developed numerical techniques to solve the equations of fluid motion and obtain three-dimensional solutions (FLOW-3D, n.d.).



Figure 2. Flowchart of the experimental model

In this project, the commercial software FLOW-3D was employed. Developed in 2000 by Flow Science, FLOW-3D is a three-dimensional (3D) hydraulic modeling program that solves the Navier-Stokes equations using numerical approximations (Flow Science, n.d.). As the most widely used commercial software for free-surface flow modeling, FLOW-3D enables precise simulations of diverse water- and environment-related engineering challenges. The software facilitates the analysis of sediment transport processes, including bedload transport, suspended sediment transport, scour, and deposition (Weig et al., 2014).

To solve a hydraulic model we have three phases: preprocessing, which refers to the input data prior to the run such as geometry, meshing in the geometry, physical properties, initial and boundary conditions; preprocessing refers to the model run and post-processing is the analysis of results.

For the calibration of the numerical model, the geometry, boundary conditions and sediment properties of the physical model were used

2.2.1 Geometry

The geometry of the physical model was imported for calibration of the numerical model of both square and circular piles.

The channel bed was modeled as a 10-cm-high solid structure, while the piles were configured as solid elements with dimensions matching the physical model. The granular material was incorporated using the packed sediment option.

2.2.2 Physical mechanisms

- Gravity - A constant force representing gravity was applied to the model, with a value of -9.81 m/s^2 along the z-axis.
- Sediment Transport - The FLOW-3D software allows the use of a sediment transport model with multiple granular sediment diameters, supporting up to 10 different particle sizes within the same bed. The model calculates particle movement through the following mechanisms (Flow Science, n.d.):

Suspension

Gravity sedimentation

Bedload transport (via bed shear stress or flow perturbations)

Bed sediment transport (rolling, sliding, or saltation)

For this model, two sediment states were considered: suspended load and bed deposit. The suspended load is transported through fluid turbulence. The FLOW-3D software displays the sediment transport model input parameters, along with the project-specific parameters selected for model calibration and final simulation. The following physical mechanisms were incorporated in the simulation calculations:

	Parámetro de ingreso	Valor o ecuación
a	Número Crítico de Shields	Soulsby-Whitehouse
b	Ecuaciones de transporte de fondo	Meyer Peter & Muller
	Coefficiente multiplicador de Richardson-Zaki	1
c	Difusión de sedimentos en suspensión	0 kg/m/s
	Multiplicador de difusión turbulenta	1.43
d	Fracción de compactación máxima	0.64
e	Relación rugosidad del lecho / D50	2.5
		0.85mm (20.4%)
f	Tipos de sedimento	0.71mm (36.7%)
		0.60mm (36.6%)
	Densidad de la partícula	2650 kg/m ³
	Coefficiente de arrastre	0.018
	Coefficiente de carga del lecho	13
	Ángulo de reposo	25 grados

✓ Critical Shields Number

The critical Shields number is a dimensionless parameter used to determine the initiation threshold of sediment motion in fluid flow (Shields, 1936). For this study, the Soulsby-Whitehouse equation (Soulsby, 1997) was selected for calculating this parameter.

$$\theta_{\text{cri}} = \frac{0.3}{1+1.2d_i} + 0.055 (1 - e^{-0.02d_i}) \quad (1)$$

Where:

$$d_i = D \left[\frac{\rho_f(\rho_i - \rho_f)g}{\mu^2} \right] \quad (2)$$

✓ Bedload Transport Equations:

For calculating bedload sediment transport, the following equations may be used:

✓ Meyer-Peter and Müller

The Meyer-Peter and Müller equation is the most widely used empirical formula for bedload transport calculation. The experimental development of this equation was conducted in sand and gravel channels using both natural and synthetic materials with grain diameters ranging from 0.4 to 30 mm (Meyer-Peter & Müller, 1948).

The Meyer-Peter and Müller equation is based on the following hypotheses (Bravo, Osterkamp, & Lopes, 2004):

The flow's capacity to transport granular bed sediment is directly related to the difference between the hydraulic shear stress acting on sediment particles and the critical shear stress required for particle motion initiation.

Energy loss is a function of the sediment's resistance to mobilization.

The flow acting on the bed reduces the tractive force available for sediment transport.

Different particle sizes are represented by the median diameter.

Unconsolidated sediment transport occurs over the bed, generating dunes and other bedforms.

Bedload transport occurs predominantly in particles with diameters greater than 0.4 mm.

✓ Nielsen

This semi-empirical equation for bedload transport calculation was developed through experiments conducted with fine-grained sediments, specifically using particle sizes smaller than those employed in the derivation of the Meyer-Peter and Müller equation (Higgins et al., 2017).

✓ Van Rijn

Empirical equation based on sediment transport experiments conducted with granular material in the size range of 0.2 to 2 mm. According to the parameters in the equation, bedload motion initiates when the effective fluid force exceeds the resistance of particles to movement (determined by weight and friction), establishing a final condition dependent on the particle angle of repose (Rijn, 1984). For materials containing significant percentages of clay or silt, cohesive effects must be considered (Rijn, 1993).

The Meyer-Peter & Müller equation was selected for bedload sediment transport calculations, as the sediment diameters used in both the physical and numerical models fall within the equation's recommended range. The equation is expressed as follows (Meyer-Peter & Müller, 1948):

$$q_{b,i} = \Phi_i \left[g \left(\frac{\rho_i - \rho_f}{\rho_f} \right) D^3 \right]^{\frac{1}{2}} \quad (3)$$

Dónde:

$q_{b,i}$ = fracción de transporte volumétrico del arrastre de fondo

Φ_i = fracción adimensional de transporte de carga del fondo

$$\Phi_i = \beta_{MPM,i} (\theta_i - \theta_{cr,i}^{\square})^{1.5} c_{b,i} \quad (4)$$

D = Diámetro de los tipos de sedimento
 ρ_f = Densidad del fluido
 ρ_i = Densidad del sedimento
g = Magnitud de la aceleración de la gravedad
 $\beta_{MPM,i}$ = coeficientes igual a 8.0 $c_{b,i}$
 θ_i = Parámetro local de Shields

$$\theta_i = \frac{\tau}{g \cdot D (\rho_i - \rho_f)} \quad (5)$$

τ = Tensión cortante de fondo

$c_{b,i}$ = fracción de volumen de material i en el lecho

- ✓ Richardson-Zaki Exponent, Suspended Sediment Diffusion, and Turbulent Diffusion Multiplier

The Richardson-Zaki exponent is a coefficient that controls the drag effect on sediment particles as they settle under increasing concentration. Its default value is 1.0.

Suspended sediment diffusion is considered when either the molecular diffusion coefficient or turbulent diffusion is defined with a non-zero value.

The turbulent diffusion multiplier, which is the inverse of the Schmidt number, is typically set at approximately 1.43 (Flow Science, n.d.).

The default software values were adopted since no specific analysis was available from the physical model regarding these coefficients.

- ✓ Maximum Packing Fraction

This parameter controls the maximum solid fraction when sediment becomes compacted. The default value is 0.64, corresponding to the maximum packing fraction for spherical particles. For polydisperse sediments, this value may increase for irregular or monodisperse sediment particles (Jurado & Oñate, 2020).

- ✓ Bed Roughness / D50 Ratio

The D50 represents the sediment size for which 50% of the material's weight consists of smaller particles. It is computed for each timestep and every sediment-containing mesh cell. The recommended multiplier for this ratio is 2.5 (Flow Science, n.d.), which has been adopted in the model.

- ✓ Sediment Types

The maximum number of sediment types that can be defined in the software is 10 (Flow Science, n.d.). The numerical model used the grain size distribution from the physical model.

For the numerical model, the three sediment sizes with the highest weight percentages were selected: 0.85 mm (20.4%), 0.71 mm (36.7%), and 0.6 mm (36.6%). Weights were entered without decimals, with the software automatically calculating percentages.

For each sediment type, naming is optional. If no name is provided, the default is "Sediment #". In this case, sieve numbers were used.

The diameter of each sediment type is defined as the mean particle size in meters.

Particle density must be specified by the user as no default value is used. The physical model used a particle density of 2650 kg/m³ (Gallardo, 2019).

The critical Shields number was calculated using the Soulsby-Whitehouse equation (Soulsby, 1997). This value can be modified cell-by-cell at each timestep to account for bed slope effects. For inclined beds, gravity introduces a tangential

force component that affects sediment stability. However, this consideration was unnecessary here given the near-horizontal bed slope.

The drag coefficient controls the sediment erosion rate under shear stress exceeding the critical value. It can scale transport rates or adjust experimental data. The default value of 0.018 (Mastbergen & Van Den Berg, 2003) was used. A value of zero disables the drag model entirely.

The bedload coefficient controls the bedload transport rate under supercritical shear stress. Values range from 5.0 for low transport to 13.0 for very high sand transport (Fernández & Van Beek, 1976). The value 13.0 was selected to match the high sand transport observed in the physical model (Chiliquinga & Pinto, 2019).

The angle of repose defines the maximum stable slope of bed material. Recommended values are 25-35° for sand and 30-40° for gravel. A value of 25° was used for the sandy bed material.

Sediment transport requires accurate shear stress estimates, necessitating a turbulence model selection (Flow Science, n.d.). The viscous fluid option with a two-equation k- ω turbulence model was implemented based on recommendations from the project "ANÁLISIS DEL TRANSPORTE DE SEDIMENTOS AGUAS ABAJO DE PANELES SUMERGIDOS APLICANDO EL PROGRAMA FLOW 3D". This followed comparative analysis of k- ϵ , k- ω and RNG models evaluating solution time, Reynolds number, and velocity profiles against experimental data (Jurado & Oñate, 2020).

The variable density model is enabled by default to compute fluid density based on suspended sediment concentration (Flow Science, n.d.).

2.2.3 Fluid selection

The selected fluid was water at 20°C with a constant density of 1000 kg/m³ and viscosity.

2.2.4 Meshing

A sensitivity analysis was performed to determine an appropriate mesh configuration, with results shown in the following table:

Table 2
Mesh Sensitivity Analysis Summary

Pila cuadrada	Malla general (m)	Malla pila (m)	Tiempo de simulación (hh:mm:ss)	Observaciones
Análisis 1	0,01	0,01	-	Modelo sin convergencia
Análisis 2	0,05	0,05	15:02:59	Mallado total de la geometría No se calibró el modelo
Análisis 3	0,05	0,01	40:00:00	Mallado total de la geometría No se finalizó la simulación
Análisis 3	0,05	0,01	15:16:23	Mallado optimizado, desde el centro de la pila 30 cm en el eje X y Y a cada lado. Se logró la calibración

The sensitivity analysis aimed to evaluate the model's behavior and response to changes in physical and numerical parameters. In this case, the goal was to optimize the model to determine the limiting mesh size that would provide results matching the calibration while optimizing simulation times. It was concluded that the optimal mesh is a structured hexahedral grid with a general size of 0.05x0.05 m and 0.01x0.01 m at the pile. The mesh was optimized to achieve shorter run times with adequate results, bringing the numerical model closer to the physical one, with errors between 0.0% and 10.0% at different times. The mesh extended 30 cm from the pile center along the X and Y axes on each side, while a 10 cm mesh was applied around the piles. Along the Z-axis, the mesh spanned from the channel bottom to 28 cm above the sand bed.

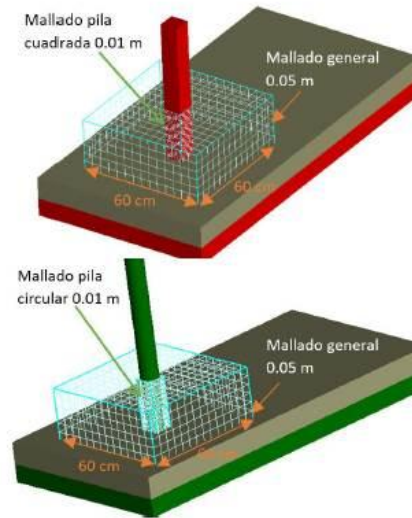


Figure 3. Mesh configuration for square and circular piles

2.2.5 Boundary conditions

The boundary conditions for the numerical model were input based on the analysis conditions established in the physical model.

X minimum. - Flow rate (Q) was set, with a constant flow rate of 52.47 l/s and a water depth of 25 cm above the sand bed surface.

X maximum. - Pressure (P) was set, with a fluid elevation of 25 cm (a condition that specifies the pressure at the outlet boundary through fluid elevation).

Y minimum, Y maximum and Z minimum. - Symmetry (S) was set so that the mesh boundaries and channel base would not interfere with the simulation results.

Z maximum. - Pressure (P) was set, with zero fluid elevation to indicate that the gauge pressure is zero at the Z maximum boundary.

An initial water depth of 25 cm above the sand bed was set to avoid sediment disturbance during flow initiation.

2.2.6 Simulation time

The simulation time is the period during which the phenomenon occurs and defines the end of the simulation. The numerical model was run for 4 hours, corresponding to the physical model's analysis time. A one-second interval was set for output results.

3 Results

3.1 Calibration

To calibrate the physical model, the maximum scour results around the pile from the numerical and physical models were compared at different times. The obtained values are presented in the following table:

3.1.1 Calibration results for the square pile

Table 3. Calibration results for the square pile

TIEMPO (HORAS)	MÁXIMA EROSIÓN (cm)		DIFERENCIA (%)
	MODELO FÍSICO	MODELO NUMÉRICO	
0	0	0	0,00%
1	5	5,5	10,00%
2	10	10,25	2,50%
3	12	11,83	1,42%
4	12	12	0,00%

The numerical model of the square pile was calibrated with a maximum difference of 10% between the physical and numerical models' maximum scour results. Figure 4 shows the sand bed level after 4 hours of modeling, with axes placed in the X and Y directions in the zone of maximum scour around the pile.

In Figure 5, the similarity in maximum scour around the square pile between the physical and numerical models is observed. The bed elevation shows a minimum value of 0.10 m around the pile, representing the channel base elevation. Therefore, the maximum scour depth is 12 cm.

3.1.2 Calibration results for the circular pile

In the numerical calibration model, it was found that the mesh used around the circular pile did not adequately integrate with the general mesh due to its shape. Several mesh attempts were made to achieve correct geometric interpretation in the mathematical space, but the model failed to converge. The computational package generated results in the general mesh that were unrelated to the results around the pile mesh. For this reason, a comparison between the physical and numerical models for calibration was not possible. The mesh separation is shown in the following figure.

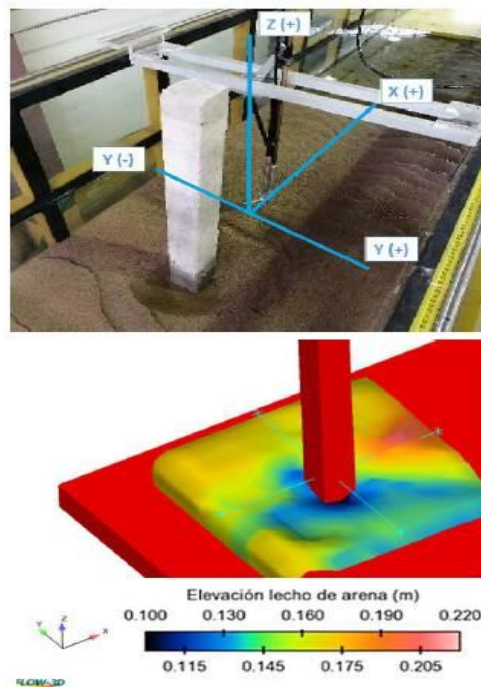


Figure 4. Numerical model calibration for the square pile

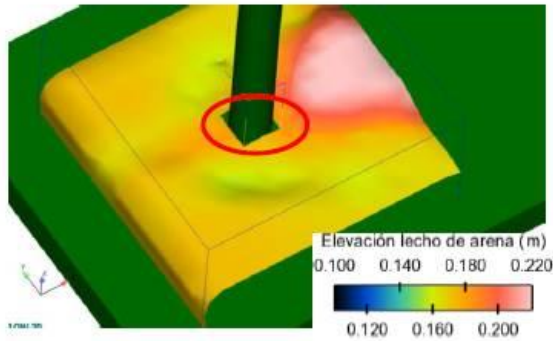


Figure 5. Numerical model for the circular pile

3.2 Improved model (Square pile)

Since the physical model could not determine the maximum scour around the pile due to the sediment bed height being limited to 12 cm, the improved numerical model used a 20 cm high bed while retaining the same geometric, physical, and boundary characteristics as the calibrated model. To evaluate the maximum scour around the square pile, the simulation time was increased to 8 hours. The results of the improved model are presented below:

Table 4. Maximum scour results around the square pile

Time (hours)	Maximum erosion (cm)
0	0
1	4,7
2	9,8
3	12
4	14,4
5	14,6
6	14,7
7	14,8
8	15

At 8 hours, the numerical model stabilized, reaching a maximum scour depth of 15 cm. In the project where the physical model was developed (Chiliquinga & Pinto, 2019), the maximum scour was estimated using empirical equations from various authors. Below is a comparison between the improved model results and the maximum scour estimates:

Table 5. Maximum scour results around the square pile

	Maximum Erosion (cm)	Difference (%)
Physical Model	15	-
Laursen and Toch Equation	20	25,00%
Maza - Sánchez Equation	18	16,67%
Melville and Coleman Equation	21,12	28,98%
CSU Equation	13,87	8,15%
Froehlich Equation	16,35	8,26%

Source: Chiliquinga and Pinto (2019)

The maximum scour result around the square pile in the physical model approximates the values calculated using the CSU and Froehlich equations, with similarity percentages of 91.85% and 91.74%, respectively.

4 Conclusion

For the numerical modeling of scour analysis around bridge piers, the computational package FLOW-3D was used. This software calculates sediment movement, predicting scour, advection, and sedimentation.

The FLOW-3D model is limited to high-performance computing workstations. Therefore, a workstation with an Intel Xeon processor (base speed of 2.2 GHz, 12 cores, 24 logical processors, 64 GB RAM, and a 4 GB graphics processor) was employed.

To determine the optimal mesh, a sensitivity analysis was conducted with different mesh sizes. The results showed that a general mesh of 0.05×0.05 m and a pier mesh of 0.01×0.01 m allowed the software to accurately interpret the pier geometry.

The numerical model of the square pier was calibrated by comparing the maximum scour around the pier between the physical and numerical models. The maximum difference was 10% at one hour and 0% at four hours.

The numerical model of the circular pier could not be calibrated because the general mesh and pier mesh did not integrate properly. It is recommended to use software that supports unstructured meshing to better adapt to circular geometries.

The numerical model of the square pier stabilized after 8 hours of simulation, yielding a maximum scour depth of 15 cm. When compared to empirical scour estimation equations, the results showed 91.85% agreement with the CSU equation and 91.74% with the Froehlich equation.

Numerical modeling allows for the accurate representation of scour phenomena around bridge piers. With this approach, we can simulate potential solutions, such as submerged panels arranged individually, in series, or in parallel at various angles of attack. These results could help mitigate bridge failures caused by hydraulic scour. Thus, this study provides a foundation for further research into potential solutions.

Conflicts of interest

The author declares no conflicts of interest regarding the publication of this paper.

References

- [1] Bravo, M., Osterkamp, P., & Lopes, L. (2004). Transporte de sedimentos en corrientes naturales. *Terra Latinoamericana*, 22(3), 377-386. <https://www.redalyc.org/pdf/573/57322315.pdf>
- [2] Chiliquina, J., & Pinto, C. (2019). *Análisis experimental en modelo físico de fenómenos de turbulencia causantes de erosión alrededor de pilas de puentes utilizando acoustic doppler velocimeter ADV [Tesis de pregrado, Escuela Politécnica Nacional]*. Repositorio digital institucional de la Escuela Politécnica Nacional. <https://bibdigital.epn.edu.ec/handle/15000/20363>
- [3] Chow, V. (2004). *Hidráulica de canales abiertos*. Nomos S.A.
- [4] Fernández Luque, R., & Van Beek, R. (1976). Erosion and transport of bed-load sediment. *Journal of Hydraulic Research*, 14(2), 127 - 144. <https://doi.org/10.1080/00221687609499677>
- [5] Fernández, M. (2004). *Estudio de la evolución temporal de la Erosión Local en*. Barcelona [Tesina]: UPCommons. <https://upcommons.upc.edu/handle/2099.1/3343>
- [6] FLOW- 3D. (s.f.). Flow 3D Hydro user manual. Obtenido de <https://C:/flow3d/HYDROv1.0u1/help/index.html>
- [7] Gallardo, K. (2019). *Demostración experimental del efecto de los paneles sumergidos en la erosión local de pilas de puentes cuadradas*. Quito, Pichincha, Ecuador [Tesis de pregrado, Escuela Politécnica Nacional]. Repositorio digital institucional de la Escuela Politécnica Nacional. <https://bibdigital.epn.edu.ec/handle/15000/20172?locale=de>

- [8] Hamad, K. (2015). *Submerged Vanes Turbulence Experimental Analysis* [Tesis doctoral, Universitat Politècnica de Catalunya]. TDX. <http://hdl.handle.net/10803/377436>
- [9] Higgins, A., Restrepo, J., Otero, L., Ortiz, J., & Conde, M. (2017). Distribución vertical de sedimentos en suspensión en la zona de desembocadura. *Latin american journal of aquatic research*, 45(4), 724-736. <http://dx.doi.org/10.3856/vol45-issue4-fulltext-9>
- [10] Jurado, L., & Oñate, V. (Julio de 2020). *Análisis del transporte de sedimentos aguas abajo de paneles sumergidos aplican. Quito, Ecuador [Tesis de postgrado, Escuela Politécnica Nacional]*. Repositorio digital institucional de la Escuela Politécnica Nacional. <https://bibdigital.epn.edu.ec/handle/15000/20172?locale=de>
- [11] Mastbergen, D., & Van Den Berg, J. (2003). Breaching in fine sands and the generation of sustained turbidity currents in submarine canyons. *Sedimentology*, 50(4), 625 - 637. <https://doi.org/10.1046/j.1365-3091.2003.00554.x>
- [12] Meyer-Peter, E., y Muller, R. (1948). Formulas for Bed-Load Transport. *Proceedings of the 2nd Meeting the International Association for Hydraulic Structures Research*, Delft, 39-64. <http://resolver.tudelft.nl/uuid:4fda9b61-be28-4703-ab06-43cdc2a21bd7>
- [13] Nielsen, P. (1992) *Coastal Bottom Boundary Layers and Sediment Transport*. World Scientific. <https://doi.org/10.1142/1269>
- [14] Rijn, Van. (1984). Sediment transport, Part I: bed load transport. *Journal of Hydraulic*, 110(10). 1613-1641. [https://doi.org/10.1061/\(ASCE\)0733-9429\(1984\)110:10\(1431\)](https://doi.org/10.1061/(ASCE)0733-9429(1984)110:10(1431))
- [15] Rijn, Van. (1993). *Principles of sediment transport in rivers, estuaries and coastal seas*. Aqua, Amsterdam Publications.
- [16] Shields, A. (1936). Application of similarity principles and turbulence research to bed-load movement. *Mitteilungen der Preußischen Versuchsanstalt für Wasserbau*. <http://resolver.tudelft.nl/uuid:a66ea380-ffa3-449b-b59f-38a35b2c6658>
- [17] Soulsby, C. (1997). Bed load transport. In *Dynamics of Marine Sand*. Thomas Telford Publications.
- [18] Weig, G, Brethour, J., Grunzner, M., y Burnham, J. (2014). The sediment Scour Model in Flow 3D. *Flow Science*.

Author Notes



Khaled Mohamed Ahmed Hamad

Hydraulic Engineering - National Polytechnic School (2015–present), Civil Engineer - Cairo University & National Polytechnic School (2008), Master of Science (MSc) in Hydraulic Engineering - National Polytechnic School (2011), and Doctor of Philosophy (Ph.D.) in Sediment Transport and Fluvial Morphodynamics - Technical University of Catalonia (UPC), Spain & University of Iowa, USA (2015). Conducted sediment transport research with Dr. Jacob Odgaard (IIHR, University of Iowa). Awarded Best Professor by the College of Civil Engineers of Pichincha at the Faculty of Civil and Environmental Engineering - National Polytechnic School (2017, 2021).



Cristina Alexandra Torres Jacobowitz

Civil Engineer, Master in Water Resources with mention in "Hydraulic Project Design" from the National Polytechnic School. Experience in design and evaluation of hydraulic structures, physical and numerical modeling of hydraulic phenomena, roadway design, programming and management of civil works. Currently works as Full-Time Occasional Professor at the Faculty of Civil and Environmental Engineering of the National Polytechnic School. Her research interests focus on: Theoretical and Computational Fluid Mechanics, Physical Modeling of Hydraulic Phenomena, Hydraulic Structure Design, and Sediment Transport.